Nanoscale Islands of the Self Assembled Monolayer of Alkanethiol

Joyanta K. Saha, Mino Yang,[†] and Joonkyung Jang[*]

Department of Nanomaterials Engineering, Pusan National University, Busan 609-735, Korea. [*]E-mail: jkjang@pusan.ac.kr
[†]Department of Chemistry, Chungbuk National University, Cheongju 361-763, Korea
Received September 21, 2013, Accepted September 27, 2013

Molecular dynamics simulations were performed to study the structure and stability of a nanoscale self-assembled monolayer (SAM) of alkanethiol on a gold (111) surface. The tilt angle and orientational order of the alkyl chains in the SAM island were examined by systematically varying the size of the island. The chain length dependence of the SAM island was examined by considering alkanethiols containing 12, 16, 20, and 24 carbon atoms. The minimum diameter of SAM islands made from 1-tetracosanethiol, 1-ecosanethiol, 1-hexadecanethiol and 1-dodecanethiol were 2.29, 1.9, 4.7 and 4.76 nm, respectively. These set the ultimate resolution that can be patterned by soft nanolithography. As the length of alkanethiol increases, the SAM islands became more ordered in both orientation and conformation of the alkyl chains.

Key Words : Self-assembled monolayer, Alkanethiol, Chain length, Nanolithography

Introduction

The self-assembled monolayers (SAMs) of alkanethiol have numerous applications as coating materials.[1] The properties of SAM can be tuned from hydrophobic to hydrophilic by manipulating the tail group of alkanethiol. These SAMs are used in molecular electronics,[2] biosensors[3] and nanofabrication,[4] as well as in other applications.[1,5,6] With the advances in soft nanolithography using scanning probes or stamps,[7,8] SAMs with widths of 10-100 nm can be fabricated on a range of surfaces.[9] In the bulk SAM on a gold (111) surface, the adsorbed sulfur atoms develop a well-ordered $\sqrt{3} \times \sqrt{3}\ R30^0$ overlayer, even at room temperature. The alkyl chains were also ordered in orientation, tilting slightly (~30°) from the surface normal.

It is unclear if the structural features of the bulk SAM, *i.e.* the dense and ordered packing of sulfur head groups and alkyl chains, will persist for the nanoscale islands of SAMs. Previously, the stability of a nanoscale SAM island of 1-octadecanethiol (ODT) on Au(111) was examined using molecular dynamics (MD) simulations. As the size of the SAM islands became a few nms in width, the SAM islands showed significant thermal fluctuations in their periphery. The minimum diameter of a stable and ordered SAM island of 1-octadecanethiol (ODT) on Au(111) was 1.9 nm (*i.e. 20* ODT molecules) at room temperature.[10]

As the stability of SAMs originate from the packing of alkyl chains (and the adsorption of sulfur headgroups to the surface), the length of alkanethiols should affect the stability. For the bulk SAMs of *n*-alkanethiols,[11-13] relatively long-chained thiols (containing 15-21 carbon atoms) form a densely packed, crystalline-like assembly. As the chain length decreases, the SAM structure will lose its compact packing and orientational order, which are characteristic of a stable SAM. This study focused on nm-sized islands of SAM and examined how the stability of the SAM islands are affected by the chain length of alkanethiols. The size-dependent structures of the nm-sized SAM islands were elucidated by examining the packing of sulfur atoms as well as the orientational order and conformation of the alkyl chain. The minimum size for a stable SAM island was estimated by systematically varying the chain length of thiol. The differences between the SAM islands and bulk SAM were discussed.

Simulation Details

The SAM islands of alkanethiols were simulated on a gold (111) surface. Four *n*-alkanethiols with different chain lengths were considered: 1-tetracosanethiol, $SH(CH_2)_{23}CH_3$, (C24 thiol), 1-ecosanethiol, $SH(CH_2)_{19}CH_3$ (C20 thiol), 1-hexadecanethiol, $SH(CH_2)_{15}CH_3$ (C16 thiol), and 1-dodecanethiol, $SH(CH_2)_{11}CH_3$, (C12 thiol).

The surface was made of two layers of 12,800 gold atoms. The CH_3, CH_2, and SH groups of *n*-alkanethiol molecules are treated as united atoms (UAs).[14,15] For each molecule, *i*, its tilt direction was defined in terms of the vector $\vec{u}_i$ (Figure 1).[15,16] To define $\vec{u}_i$ for each molecule, *i*, seven UAs, which have odd numbers of intervening CH_2 groups between them and the S atom, were selected. $\vec{u}_i$ was defined as the average of the direction vectors from the S atom to these selected UAs. The tilt angle, θ_i, of the ith molecule is given by the polar angle of $\vec{u}_i$ relative to the surface normal. The backbone plane orientation of the alkanethiol molecules is described by the following vector (for the case of the C16 thiol),

$$\vec{b}_i = \sum_{j=1}^{13} (-1)^j \vec{r}_j \qquad (1)$$

where $\vec{r}_i$ is the jth C-C bond vector starting from the S atom. $\vec{b}_i$ is the average of the vectors, which dissect the C-C-C or C-C-S angles and lie on the planes defined by these triplets.
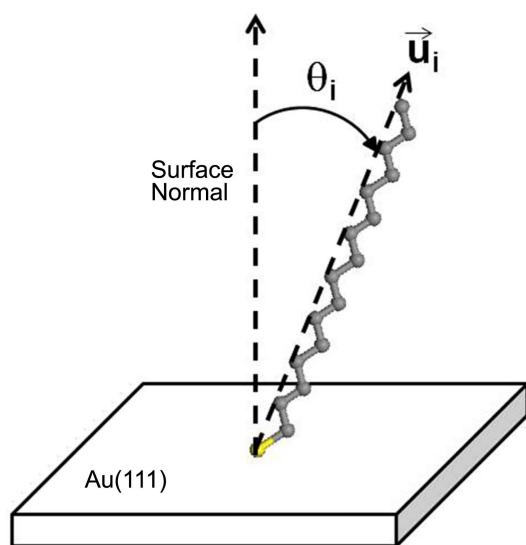
Figure 1. Diagram of the orientation of 1-hexadecanethiol (C16 thiol). Shown is an C16 thiol molecule with all-trans conformations. The tilt angle, θ_i, is the polar angle of the tilt direction vector, $\vec{u}_i$, measured from the surface normal.

In calculating $\vec{u}_i$ and $\vec{b}_i$, the three UAs at the tail of the chain were excluded because these contain many gauche defects. $\vec{u}_i$ and $\vec{b}_i$ were also normalized as unit vectors. The ordering in the molecular orientation was quantified by the order parameter,[17]

$$O_X = \langle 0.5[(\vec{X}_i \cdot \vec{X}_j)^2 - 1]\rangle_{i \neq j}, \qquad (2)$$

where $\langle \rangle_{i \neq j}$ represents the average over all intermolecular pairs and $\vec{X}_i = \vec{u}_i$ or $\vec{b}_i$.

The bond stretching and bending angle interactions between the UAs were modeled by the harmonic potentials.[18] The four-atom torsion potential (C-C-C-C or C-C-C-S) was modeled using a triple cosine function of the dihedral angle, ϕ, where $\phi = \pm 180°$ and $\phi = \pm 60°$ correspond to the trans and gauche conformations, respectively.[19] All the non-bonded interactions were considered to be the Lennard-Jones (LJ) potentials,

$$V_{LJ}(r) = 4\varepsilon\left[\left(\frac{\sigma}{r}\right)^{12} - \left(\frac{\sigma}{r}\right)^6\right], \qquad (3)$$

where r is the interatomic distance and ε and σ are the LJ energy and length parameters, respectively.[15] The Lorentz-Berthelot combination rules[20] were used for the LJ parameters of the hetero atomic pairs. The S-Au pair interaction was modeled using the Morse potential,[21]

$$V_{Au-S}(r) = D_e \exp[-\alpha(r - r_e)]\{\exp[-\alpha(r - r_e)] - 2\}, \qquad (4)$$

where D_e and r_e are the well depth and the distance at the minimum of the potential energy, respectively. The LJ and Morse parameters were taken from previous simulations.[10,22,23] Further details of the present model is described elsewhere.[22]

MD simulations were run by fixing temperature at 300 K using the Berendsen thermostat.[25] The time propagation was performed using the velocity Verlet algorithm with a time step of 1 fs. The positions of all the Au atoms were fixed throughout simulation. The periodic boundary conditions were applied with a minimum image convention[20] by using the lateral lattice vectors of (19.58 nm, 11.54 nm, 0) and (0, 23.07 nm, 0).

The number of molecules comprising the SAM island, N_{thiol}, was varied from 10 to 50. A circular SAM island was prepared, where fifty of the C24 thiol molecules stand up and their S atoms form a $\sqrt{3} \times \sqrt{3} R30°$ overlayer on a Au (111) surface.[6] This SAM island was then equilibrated for 20 ns in the simulation. The molecules at the periphery were then removed to produce circular SAM islands consisting of 45, 40, 35, 30, 25, 20, 15 and 10 molecules. This procedure was followed for four different alkanethiol molecules (C24, C20, C16 and C12 thiol). A 10 ns long MD simulation was run for each SAM island ($N_{thiol} = 10$-50), but the initial 100 ps was discarded for equilibration. The DL POLY package[26] was used to implement these MD methods.

The diameter of a SAM island was estimated by selecting the S atoms at the periphery and then calculating their distances from the center of the S atoms. A S atom at the periphery was defined as one with less than six neighboring S atoms within a distance of 5.5 Å from it. The average SAM diameter was calculated by taking an average over 800 MD snapshots.

Results and Discussion

The representative MD snapshots of the SAM islands made of thiols with different lengths were examined. In Figure 2, the side (left) and top (right) views are shown for the SAM islands of the C24, C20, C16, and C12 thiol molecules. Each SAM island consisted of 50 molecules. As in the bulk SAM, the S atoms develop a $\sqrt{3} \times \sqrt{3} R30°$ overlayer and the molecules stand up with their chains packed together and slightly (~20°) tilted away from the surface normal. Owing to thermal motion, however, some of the chains at the periphery were not straight, but folded, and their S atoms departed from the hexagonal close packing (but they recover original positions soon). Another feature of these nanoscale SAM islands is that the tilt direction of the chain was not uniform. The tilt direction varied either clockwise or counterclockwise (see the top views of the snapshots shown in Figure 2).

As the SAM islands decrease in size, stabilization due to the inter-chain packing diminishes and the islands become unstable. As shown in Figure 3, the SAM islands made from 10 molecules did not show the compact hexagonal packing of S atoms. The S atoms move significantly, whereas the alkyl chains entangled together, and the island diffuses as a whole over the surface. The alkyl chains are neither upright nor densely packed with each other. The chains constantly fold and unfold.

A range of structural parameters were examined by varying the number of molecules comprising the SAM island N_{thiol}. Figure 4 shows the mean distance between the neigh-
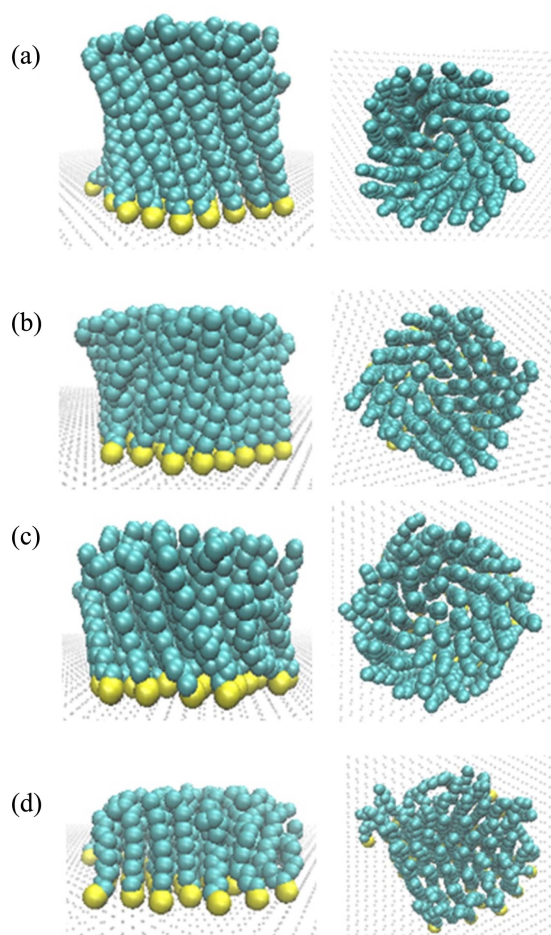
Figure 2. Snapshots of the SAM islands of thiols with various lengths. Drawn are the top (left) and side (right) views of the SAM islands made from the C24 (a), C20 (b), C16 (c), and C12 (d) thiols. Each SAM island consists of 50 molecules. The gold atoms are drawn as dots.
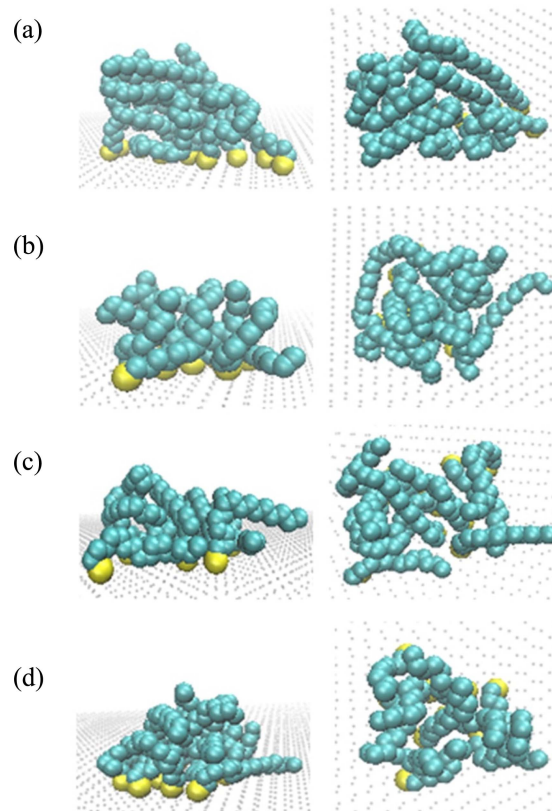

Figure 3. Unstable SAM islands of alkanethiols with different lengths. Drawn are the SAM islands made of the C24 (a), C20 (b), C16 (c), and C12 (d) thiols, respectively. The right (left) panels show the top (side) views. Each SAM consists of 10 molecules. The gold atoms are drawn as dots.
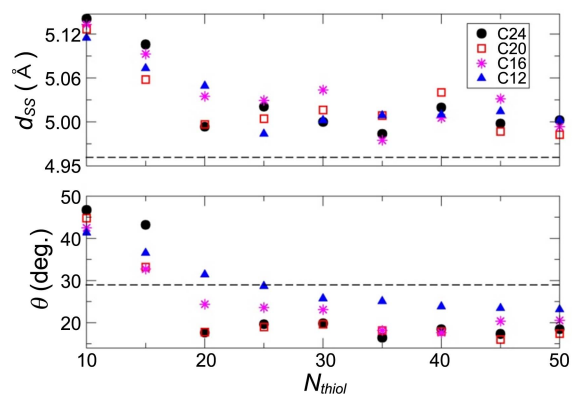

Figure 4. The average distance between the neighboring sulfur atoms d_{SS} (top) and the average tilt angle of alkyl chains from the surface normal θ (bottom) *vs.* the number of molecules comprising the SAM island N_{thiol}. Drawn as broken lines are the values for the bulk SAM of ODT.

boring S-S pairs d_{SS} (top) and the average tilt angle θ (bottom) *vs.* N_{thiol}. For comparison, the values of the bulk SAM of ODT were drawn as horizontal broken lines.[10] With increasing N_{thiol}, d_{SS} decreased and converged to ~4.8 Å at $N_{thiol} = 20$, regardless of the chain length. This means that the SAM island establishes the compact packing of sulfur atoms with increasing island size, starting at $N_{thiol} = 20$. In addition, the packing of sulfur atoms is largely independent of the chain length. The packing of sulfur atoms for the present SAM islands is not as compact as for the bulk SAM of ODT, because the converged d_{SS} values are greater than the value of the bulk SAM (~4.5 Å, drawn as the broken line).

The tilt angle also decreased and leveled off with increasing N_{thiol}. In the cases of the C24 and C20 islands, leveling off occurred near $N_{thiol} = 20$. In contrast, for the two short thiols, the C16 and C12 thiols, the plateau in the tilt angle reached at a larger value of N_{thiol}; 35 and 40, respectively. This behavior contrasts with that found for d_{SS} *vs.* N_{thiol}, where the plateaus occurred at $N_{thiol} = 20$. Therefore, the tilt angle depends on the chain length. Note that the converged values of θ (18.5º, 17.4º, 20.6º, and 23.1º for the C24, C20,

C16, and C12 islands, respectively) with increasing N_{thiol} are smaller than the bulk value (broken line). Therefore, chains of the present SAM islands are less tilted from the surface normal than those of the bulk SAM.

The conformation of alkyl chains was also checked by varying the size of the SAM island. In Figure 5, the percentage of the trans conformation *vs.* N_{thiol} was plotted.
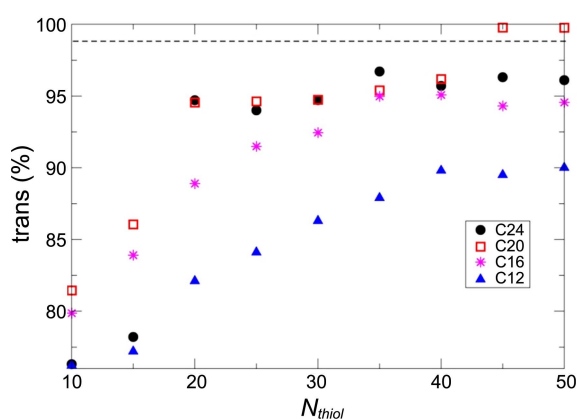
Figure 5. Conformation of the alkyl chains of the SAM island. Plotted is the percentage of trans conformation *vs.* N_{thiol} for four different thiols. The percentage of trans conformation of the bulk SAM of ODT is drawn as the broken line.

Figure 6. Ordering of the tilt direction and the backbone plane orientation in the SAM island. The order parameters of the tilt orientation O_u (top) and backbone plane orientation O_b (bottom) are plotted *vs.* N_{thiol}. For comparison, the O_u and O_b values of the bulk SAM of ODT are shown as broken lines.

Regardless of the chain length of thiol, the percentage of the trans conformation increased and converged with increasing N_{thiol}. Convergence occurred at $N_{thiol} = 20$ for the C24 and C20 thiols, but the plateau for the C16 and C12 SAM islands reached at $N_{thiol} = 35$ and 40, respectively. Except for the shortest thiol, the percentage of the trans conformation in the SAM island reached ~95% or more with increasing N_{thiol} (~100% for the C20 islands with $N_{thiol} = 45$ and 50). The trans percentage for the C12 island reached up to 90% with increasing island size. Overall, the percentage of the trans conformation for these SAM islands was smaller by 5% or more than that of the bulk SAM (drawn as the broken line).

Finally, the size dependence of the orientational order of the alkyl chains in the SAM island was inspected. Figure 6 (top) shows the order parameter of the tilt direction, O_u, as a function of N_{thiol}. Regardless of the length of thiol, O_u, increases and plateaus with increasing N_{thiol}. All the plateau values were smaller than the value for bulk SAM. For the C24 and C20 SAM islands, the plateau of O_u was reached at $N_{thiol} = 20$. The plateau of O_u for the C16 and C12 SAM islands was reached at $N_{thiol} = 35$ and 45, respectively. These N_{thiol} values, where convergence occurs, coincide with those found for the size dependence of the tilt angle θ and the trans conformation. The converged O_u with increasing N_{thiol} for the C24 and C20 islands was almost 0.77, which is larger than the value for the two short-chained thiols (C16 and C12 thiols). The chain orientation for the two long thiols was more ordered than that of the two short chained thiols. Note also the orientational ordering of the present SAM islands was less complete than that of the bulk SAM (broken line, $O_u = 0.98$).

Regarding the backbone plane orientation, the O_b values also increase and level off with increasing N_{thiol} (Figure 6, bottom). The converged O_b values for the SAM islands were less than the value for the bulk SAM (0.24). The O_b values were much lower than the corresponding O_u values, suggesting that the backbone plane orientation is not as ordered as the tilt direction. For the C24 and C20 thiol islands, O_b increased sharply near $N_{thiol} = 20$, whereas it increased
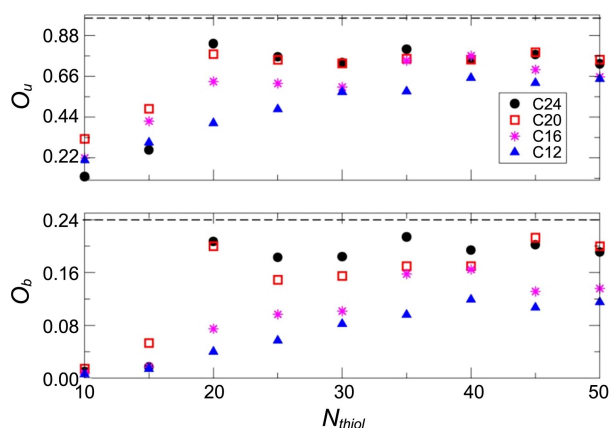
gradually and leveled off at $N_{thiol} = 35$ and 40, respectively, for the C16 and C12 islands.

In summary, the structure and stability of SAM islands, a few nms in width were examined by systematically varying the size and chain length of the island. Regardless of the length of chain, as the size of the SAM island increased, the structure of the islands approached that of the bulk SAM. An examination of the packing of S atoms and the chain conformation and orientation showed that the structure of the SAM island becomes stable if the number of molecules is greater than 20 for the C24 and C20 thiols. For the short thiols considered, the C16 and C12 thiol, respectively, the number of molecules required for a stable island increased to 35 and 40.

Conclusion

Molecular dynamics simulations were used to examine the small size limit of SAM islands made from alkanethiol chains with various lengths. This limit is related to the ultimate resolution of the SAM patterns fabricated by soft nano-lithography. The structure of the SAM island was studied by examining the tilt angle, conformation, and orientational ordering of alkyl chains, as well as the packing of the sulfur head groups. As the number of molecules comprising the SAM islands exceeds a certain value, the structure of island became stable, resembling the well-ordered bulk SAM. An examination of the structural parameters above showed that 20 molecules are needed to form an upright and ordered SAM made of the C24 and C20 thiols. For the C16 and C12 thiols, it took 35 and 40 molecules, respectively, to establish a robust SAM island. Depending on the length of thiol, however, there were some differences in these stable SAM islands. The islands of short thiols were more tilted from the surface normal and had a lower percentage of the trans conformation. The shortest two thiols showed less orientational ordering of the alkyl chains than that for the two longest chained thiols.

References

1. Love, J. C.; Estroff, L. A.; Kriebel, J. K.; Nuzzo, R. G.; Whitesides, G. M. *Chem. Rev.* **2005**, *105*, 1103.
2. Mirkin, C. A.; Ratner, M. A. *Annu. Rev. Phys. Chem.* **1992**, *43*, 719.
3. Sackmann, E. *Science* **1996**, *271*, 43.
4. Piner, R. D.; Zhu, J.; Xu, F.; Hong, S.; Mirkin, C. A. *Science* **1999**, *283*, 661.
5. Silverberg, M. *J. Chem. Phys.* **1993**, *99*, 9255.
6. Ulman, A. *Chemical Reviews* **1996**, *96*, 1533.
7. Salaita, K.; Wang, Y.; Fragala, J.; Vega, R. A.; Liu, C.; Mirkin, C. A. *Angew. Chem. Int. Ed.* **2006**, *45*, 7220.
8. Gates, B. D.; Xu, Q.; Stewart, M.; Ryan, D.; Willson, C. G.; Whitesides, G. M. *Chemical Reviews* **2005**, *105*, 1171.
9. Manandhar, P.; Jang, J.; Schatz, G. C.; Ratner, M. A.; Hong, S. *Phys. Rev. Lett.* **2003**, *90*, 115505.
10. Saha, J. K.; Ahn, Y.; Kim, H.; Schatz, G. C.; Jang, J. *J. Phys. Chem. C* **2011**, *115*, 13193.
11. Nishi, N.; Hobara, D.; Yamamoto, M.; Kakiuchi, T. *J. Chem. Phys.* **2003**, *118*, 1904.
12. Nuzzo, R. G.; Korenic, E. M.; Dubois, L. H. *J. Chem. Phys.* **1990**, *93*, 767.
13. Porter, M. D.; Bright, T. B.; Allara, D. L.; Chidsey, C. E. D. *J. Am. Chem. Soc.* **1987**, *109*, 3559.
14. Ghorai, P. K.; Glotzer, S. C. *J. Phys. Chem. C* **2007**, *111*, 15857.
15. Hautman, J.; Klein, M. L. *J. Chem. Phys.* **1989**, *91*, 4994.
16. Bhatia, R.; Garrison, B. J. *Langmuir* **1997**, *13*, 4038.
17. Fujiwara, S.; Sato, T. *J. Chem. Phys.* **1999**, *110*, 9757.
18. Jorgensen, W. L.; Maxwell, D. S.; Tirado-Rives, J. *J. Am. Chem. Soc.* **1996**, *118*, 11225.
19. Jorgensen, W. L.; Madura, J. D.; Swenson, C. J. *J. Am. Chem. Soc.* **1984**, *106*, 6638.
20. Allen, M. P.; Tildesley, D. J. *Computer Simulation of Liquids*; Oxford University Press: New York, 1987.
21. Zhao, X.; Leng, Y.; Cummings, P. T. *Langmuir* **2006**, *22*, 4116.
22. Ahn, Y.; Saha, J. K.; Schatz, G. C.; Jang, J. *J. Phys. Chem. C* **2011**, *115*, 10668.
23. Hautman, J.; Klein, M. L. *J. Chem. Phys.* **1989**, *91*, 4994.
24. Berendsen, H. J. C.; Postma, J. P. M.; van Gunsteren, W. F.; DiNola, A.; Haak, J. R. *J. Chem. Phys.* **1984**, *81*, 3684.
25. Smith, W.; Yong, C. W.; Rodger, P. M. *Mol. Simul.* **2002**, *28*, 385.